Replicating the activation time of electronically controlled watermist system nozzles in B-RISK

M. Spearpoint [a],[*], C. Hopkin [b], Y. Muhammad [c], W. Makant [c]

[a] *OFR Consultants, Manchester, UK*
[b] *Ashton Fire, Manchester, UK*
[c] *Plumis Ltd., London, UK*

ABSTRACT

This paper presents two series of enclosure fire experiments in which the activation time of electronically controlled watermist system nozzles and concealed sprinklers have been obtained. The first series experiments were aligned to the procedure given in the BS 8458 standard whereas the second series were configured to give slower growing fires than in the standard test.

The activation of the two systems have been simulated in the B-RISK zone fire model. Activation characteristics for the concealed sprinklers have been taken from elsewhere in the literature. Representative activation characteristics for the electronically controlled watermist system nozzles have been determined. The selection of these characteristics has required a balance between the results from the two experimental series. By using an effective response time index of 20 $\mathrm{m}^{1/2}\mathrm{s}^{1/2}$ and an effective conductivity factor of 0.25 $\mathrm{m}^{1/2}\mathrm{s}^{-1/2}$ the predicted activation times are on average 14% slower across all of the enclosure fires.

1. Introduction

1.1. Background

A report on a recent a study on the causes of fire fatalities and serious fire injuries in Scotland and potential solutions to reduce them [1] suggested that "*More needs to be done in terms of reliable early detection and suitable intervention, to either delay the development of the fire or to notify people – using technology – so they can take suitable action at the early stages of the fire.*" Automatic water fire suppression systems (AWFSS), such as sprinklers and watermist, provide a means to protect lives and property by both detecting a fire and then controlling or extinguishing it.

Shielded fire scenarios present a challenge to suppression systems when compared to cases in which the fire is open to the suppression medium. In the report by BRE [2] it was noted that "*Sprinkler protection was not found to be a complete panacea, slow-growing and shielded fires can be a problem.*" Similarly, previous work by Grosshandler et al. [3] on using water mist to protect computer cabinets found that suppressing these fires in obstructed locations is challenging.

This paper reports on two series of enclosure experiments in which the activation of a watermist system with electronically controlled nozzles has been measured. Series A consisted of BS 8458 [4] fire test configurations and Series B were ad-hoc enclosure experiments in which the fire source was configured to give a longer development time in

comparison with those in Series A, as well as considering the impact of shielding the fire. In addition to the watermist system, the Series B experiments also included measuring the activation time of concealed residential sprinkler heads.

In this paper the measured activation times of the watermist system and the concealed sprinklers have been compared. The B-RISK zone model [5] has then been used to reproduce the experiments as closely as possible, comparing simulation outputs to data for system activation time. As part of this, representative thermal sensitivity properties for the watermist system have been identified through a parametric analysis, assuming that the system can be represented as an equivalent sprinkler head. For the concealed sprinkler heads, the activation properties have been taken from the previous work of Hopkin and Spearpoint [6], with the aim to verify whether their recommended design parameters for concealed heads align with the experiments.

1.2. Electronically controlled nozzles

The concept of using an electronic means of activating a AWFSS rather than using the traditional thermally responsive elements has been discussed in the literature. Magnone et al. [7] consider the challenges posed by modern warehouse storage requirements and how ceiling-only mounted sprinklers that are electronically activated by detection and control system can provide a viable suppression solution. Kopylov et al.

---

[8] present a technique to modify conventional sprinklers so that they can be enforced to activate using an electrically powered heating arrangement. Similarly, there are watermist systems available on the market which do not operate in the same way as traditional mist systems, either in their activation methods, nozzle arrangements, or how they introduce water droplets into the fire-affected enclosure.

The focus of this paper is a specific watermist system which incorporates electronically controlled nozzles (referred to hereafter as an 'electronic nozzle system') instead of nozzles which are heat activated. For this system, the nozzle is activated by a linked wireless/wired smoke or heat (or combined smoke and heat) detector. Following this activation, the system uses an infrared (IR) thermopile sensor located within the nozzle head(s) to scan the enclosure. When scanning the enclosure, the IR sensor measures temperature as a function of IR radiation, assessing for high temperature readings or differential increases in temperature between scans. Once the temperature exceeds a given threshold, the head is deemed to have successfully located a fire and discharges water droplets in the direction of where the high temperature readings have been observed. The water is discharged by the activation of a high-pressure pump, driving water fed from a reticulated supply through the nozzle unit, with the nozzle achieving a water rate discharge of around 5.6 L/min.

The electronically controlled nozzles are wall mounted and positioned around light switch height, e.g. 1.45 m from floor level. In positioning the heads at this height, the intent is for the water spray to be entrained in the fire plume and to minimise what is deemed to be 'ineffective' evaporation in the upper, hot smoke layer. A visualisation of the system configuration is presented in Fig. 1 and further information including application guides, test reports and case studies is available from the supplier [9].

There are several motivations behind the development of automatic nozzle watermist systems as an alternative to existing suppression methods. The first is that, by adopting a method of activation linked to a smoke detector and an IR sensor, a quicker response time might be expected compared to a conventional system, which is typically reliant on substantial development of heat in the fire plume and subsequent heat transfer to the sensing element. By providing quicker detection and system activation, this has the potential to suppress the fire earlier in its development, reducing the hazard for occupants. The fire location identification capability of the system has undergone extensive development and assessment to minimise the effects of false signals from IR sources such as heating systems, candles etc. Details of this work are outside the scope of this paper.

Another motivation relates to the introduction of finer water droplets and thus a lower rate of water discharge, minimising any requirement for large water tanks to support the system's operation. This approach also provides greater flexibility for the retrofitting of systems, enhancing
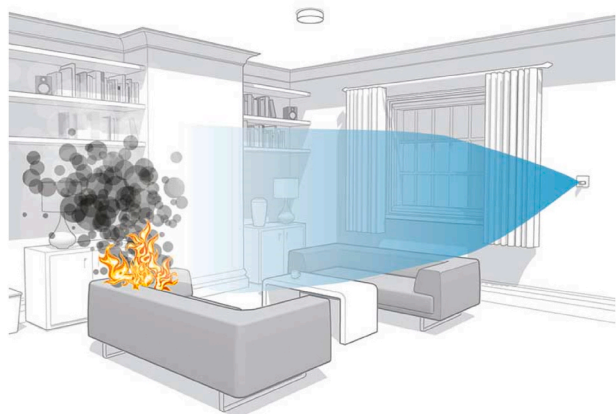

Fig. 1. Visualisation of the electronically controlled nozzle system configuration with a nozzle discharging water towards a fire.

the safety of existing buildings. However, these motivations are conceptual and require validation for whether system is adequate in its intended purpose.

Much of fire safety engineering design is based on historical approaches. The introduction of novel methods and systems can be met with an understandable level of scrutiny, with a common expectation that any new system should be able to achieve an equivalent level of safety to an existing system that meets the relevant standard, irrespective of the intended performance target. Furthermore, the comparisons made between conventional and new systems tend to be evaluated in the context of 'legacy' hazards, without necessarily considering how hazards may change over time. The harmonisation of test standards for these legacy hazards can then be used as evidence, unintentionally or otherwise, that a system is suitable for a broader range of hazards.

Therefore, the research presented in the paper is part of a wider project to examine how an electronically controlled nozzle system performs in comparison to traditional sprinkler systems, as well as considering its impact on hazards which are not currently captured in existing standard test methods. Efforts are also being made to provide fire engineers with the input parameters and assumptions necessary to represent these systems in performance-based assessments. As a result of the system's operational steps it would be a complex task to represent these interactions in a computational model. For example, determining when the detector activated would not include the time required for the location of the fire by the IR sensor. Instead, the objective of this work is to examine whether a set of 'effective' sprinkler head properties can be obtained that provide a practical engineering approach to calculate the system response time.

2. Description of experiments

2.1. Series A

2.1.1. Enclosure configuration and suppression system

In Series A the electronic nozzle system was tested by an independent laboratory to Annex C of the British Standard BS 8458 [4]. The system included a wirelessly linked smoke/heat detector in the centre of the enclosure and was operated as described in Section 1.2. For the specific nozzle arrangements that were tested, the system was able to successfully achieve the acceptance criteria for watermist systems with automatic nozzles.

The BS 8458 test room is 8 m long by 4 m wide by 2.5 m high with the fire placed in three different locations, as indicated in Fig. 2. The presence of the plywood panels provided a measure of concealment from the activation sensors. BS 8458 [4] Annex C specifies that the room ceiling should be covered by 12.5 mm thick Type F fire-rated plasterboard conforming to BS EN 520:2004 [10].

2.1.2. Fire source

For the BS 8458 tests, the following arrangement and fire 'packages' are adopted:

- The 'ignition package' comprises a steel tray which is 300 mm wide by 300 mm long by 100 mm high, containing 200 mL of heptane floated on water. A wood crib is placed on top of the tray (with an optional lip added to the tray to provide stability to the crib), consisting of eight layers of wood sticks (pinus sylvestris), with each layer being four sticks spaced 50 mm apart. Each individual stick is 38 mm by 38 mm cross-section with a length of 305 mm (see Fig. 6(a) later). The complete wood crib achieves nominal dimensions of 305 mm by 305 mm by 305 mm with a combined mass of 8250 g ($\pm$250 g). Two 250 mm long cotton wicks, soaked in 100 mL of heptane, are placed on a fire brick, with 150 mm laid along the edge of the foam sheets.

- The 'ignition package' is arranged next to the 'fuel package' which consists of two sheets ('slabs') of polyether foam with dimension 865
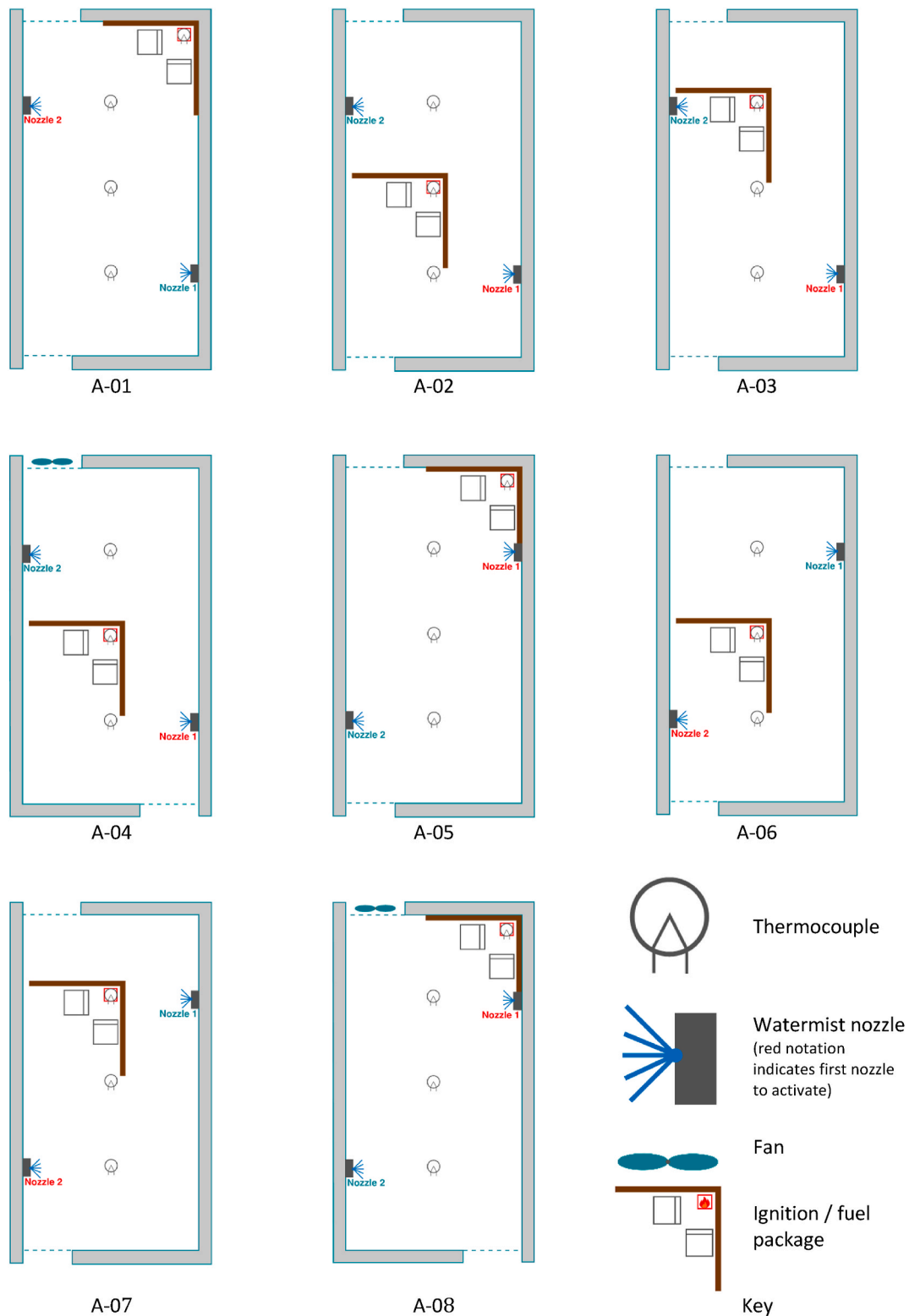
Fig. 2. Series A configurations.

mm long by 775 mm wide by 75 mm thick having a density of 20 kg/m^3. Each sheet is glued to a sacrificial backing board of the same width and length and a depth of 12 mm. This backing board is then attached to a wooden supporting frame. The foam sheets are flush with the top and sides of the sacrificial board and frame.

- In addition to the ignition and fuel package, test arrangements also incorporate plywood panels:

For a corner fire test, two walls are covered floor to ceiling by 12 mm thick plywood panels, covering a length of 2.4 m (Fig. 3). The ignition and fuel packages are placed 50 mm from the panels. For a centre fire test, a partition arrangement of plywood panels is used, again 12 mm thick but with a length of 2.2 m and a height of 1.2 m. As with the corner test, the packages are placed 50 mm from the panels.
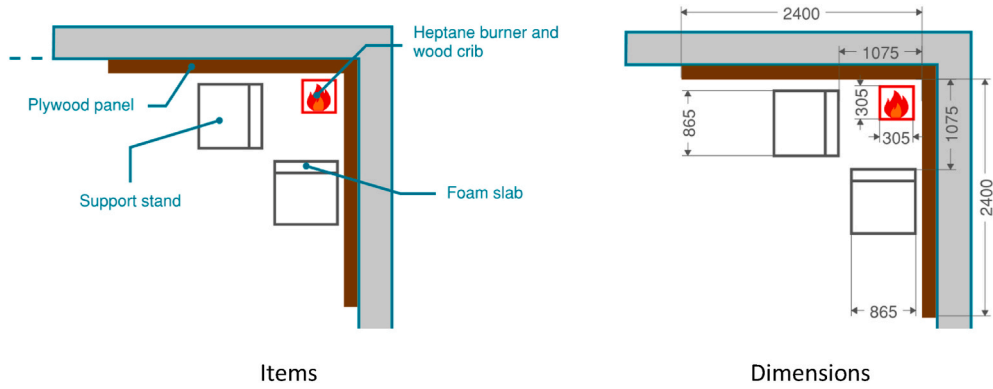
Fig. 3. Ignition and fuel package arrangement (in the corner). All dimensions in mm.

The ignition and fuel package arrangement is consistent with those used in BS 9252 [11], BS EN 12259–14:2020 [12] and UL 1626 [13] fire tests for residential sprinklers.

The heat release rate (HRR) for the BS 8458 fire test is neither defined nor measured during the testing procedure. Bill et al. [14] note that the ignition and fuel package are not sufficiently specified to provide a 'reproducible test', and thus that each test could potentially provide a wide range of growth times and maximum HRRs. This can therefore cause difficulty in estimating fire parameters for simulations of the tests.

In their investigation of human tenability when subject to a fire load equivalent to the UL 1626 'corner fire', Hostikka et al. [15] discuss previous full-scale laboratory measurements by UL, where the HRR for the corner fire was described as being initially around 100 kW, increasing in a t^2 manner to 300–500 kW after 60 s and then reaching 1500 kW in 80–95 s. The HRR curve described by Hostikka et al. is presented in Fig. 4, for a midpoint and upper/lower bound. However, Hostikka et al. do not define what maximum HRR is likely to be reached by the fuel package. The ignition and fuel package arrangement used in the UL 1626 fire test is consistent with that used in the BS 8458 test (noting that the foam used in the UL test is specified as 27–30 kg/m^3 versus 20 kg/m^3 in the BS test), and therefore it is reasonable to assume the HRR described by Hostikka et al. aligns to the BS 8458 test fire, although the comments of Bill et al. with respect to reproducibility are heeded. From the relationship described by Hostikka et al., in the initial

stages of fire development, the fire growth appears to sit somewhere between a standard Fast and Ultra-fast t^2 fire.

Elsagan and Ko [16] undertook numerical modelling of watermist systems and the BS 8458 fire test using the Fire Dynamics Simulator (FDS) [17] computational fluid dynamics (CFD) tool, using FDS to estimate the HRR curves, also presented in Fig. 4. These curves represent the estimated HRR prior to any system activation. In comparison to the HRR described by Hostikka et al., Elsagan and Ko estimated as much faster fire growth rate, with a maximum HRR in the region of 2500–6000 kW, the latter being specifically for a timber enclosure. Elsagan and Ko make no comparison of their representation of the HRR with any experimental results, so it is difficult to ascribe confidence in their results.

2.2. Series B

2.2.1. Enclosure configuration

In Series B the room geometry consisted of two inter-connected enclosures, each 4.0 m by 4.0 m by 2.5 m high (Fig. 5). The two enclosures were linked by a door opening (2.1 m high by 0.9 m wide). A second door was placed in the wall of the enclosure remote from the fire to allow access but was closed during the experiments. The enclosure walls and ceilings were made of 12 mm thick standard 4 m × 2 m plasterboard on standard wood stud and the floor was solid concrete.

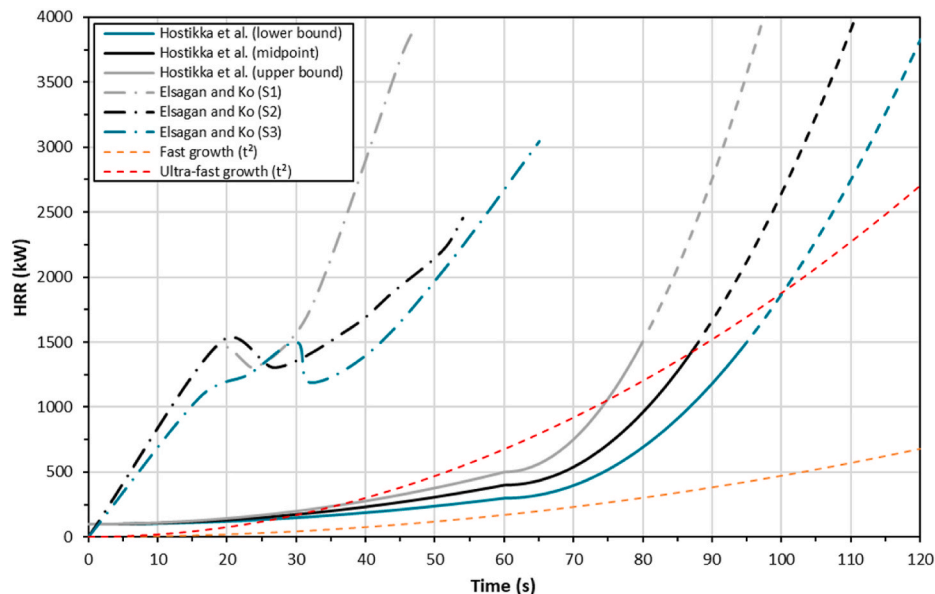Instrumentation consisted of thermocouples, optical density meters,

Fig. 4. HRR plots for fire test ignition/fuel package, derived from previous studies (S1 to S3 are the three simulation runs carried out by Elsagan and Ko).
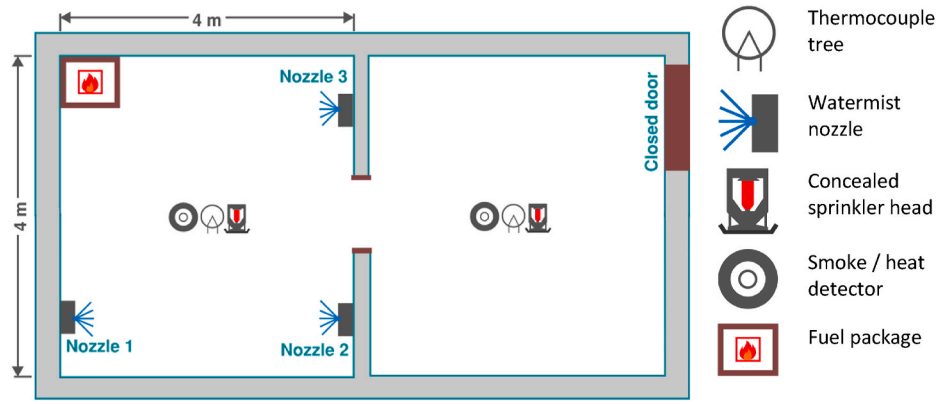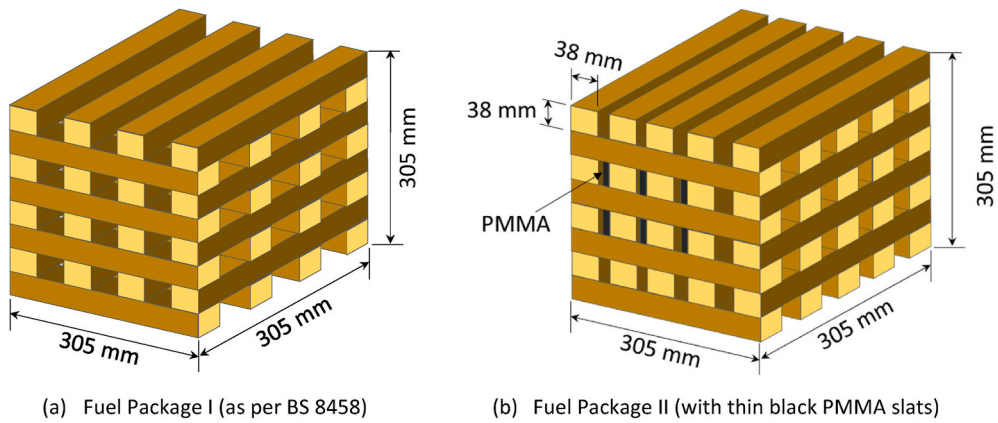
Fig. 5. Series B experimental setup.

(a) Fuel Package I (as per BS 8458)

(b) Fuel Package II (with thin black PMMA slats)

Fig. 6. Crib arrangements (not to scale).

and toxic gas species measuring equipment for carbon monoxide (CO) and carbon dioxide (CO_2) although for the purposes of this paper a detailed description is not provided herein.

2.2.2. Fire source

Five experiments were conducted for Series B. The fuel packages were selected to relate to the BS 8458 test in terms of the use of a similar crib arrangement, but the objective was to have a much slower fire

Fig. 7. Simulated fridge in the corner of the room (left) and load cell loaded with Fuel Package I (right).

growth. Therefore, the heptane and foam slabs were not incorporated in this series.

Experiment B-01 used a wood crib conforming to that used in the BS 8458 test. For the other experiments in Series B the arrangement was modified to include an additional stick per layer to create a crib in which the fire would develop more slowly than that used in BS 8458. In addition, six 6 mm thick by 38 mm tall by 305 mm long strips (0.48 kg per strip) of polymethyl methacrylate (PMMA) were included (see Fig. 6) to increase the smoke production when compared to only using wood. The concept of incorporating the PMMA was similar to the approach of Rappsilber and Krüger [18] for mixed-material cribs although in this work the proportion of PMMA compared to wood was less and the strips were oriented vertically rather than at an angle. The cribs were placed on a load cell to measure the mass loss. The crib was ignited by lighting two wicks soaked in heptane laid at the two neighbouring front corners of the crib.

The crib and load cell arrangement were located in one corner of the enclosure, away from the inter-connecting door. In all but one of the experiments the crib was placed inside a box to represent an electric appliance (such as a refrigerator) to create a shielded fire scenario. The box was made from steel and lined with 12 mm thick plasterboard and was 1800 mm tall by 670 mm deep and 800 mm wide (Fig. 7). The box was enclosed on three sides and at the top. The remaining experiment had the crib placed in the same location but without the box.

2.2.3. Suppression systems

In four of the experiments a single residential concealed sprinkler was positioned on the ceiling in the nominal centre of the fire enclosure. The electronic nozzle system was setup and operated as it would in a practice, in the manner described in Section 1.2. The combined IR sensor and watermist nozzles were arranged at three wall locations (Fig. 5) to provide a detailed assessment of the system performance.

In two experiments the fire was allowed to continue burning without any suppression after system activation whereas suppression was initiated after activation in the other four experiments. Of these four experiments, suppression was by the residential sprinkler in two cases and by the watermist nozzles in the other two cases. Details of the suppression is not provided herein as this paper is focussing solely on the activation time. The Series B experimental parameters and results discussed in Section 4.2, and summarised in Table 5.

3. Simulation methodology

3.1. Overview

A significant body of research has gone into quantifying the activation of sprinklers and how they interact with a fire. However, electronic nozzle systems operate in a unique manner when compared to traditional sprinkler systems and even typical water mist systems in (a) how the first activate and (b) how they introduce water droplets into the fire affected enclosure. This novelty can introduce complications should fire engineers ever wish to undertake computational modelling assessments to represent its impact on a design fire scenario.

To assist in the development of design input parameters for point (a) above, the primary focus of the simulations is to determine reasonable thermal sensitivity parameters which can be used to represent the activation of the electronic nozzle system as an equivalent residential sprinkler system. To do this, the modelling attempts to reproduce the experiments as closely as possible. This provides a means of representing the electronic nozzle system using existing methods, without requiring any significant modifications to the fire models and tools which are used.

A zone modelling approach has been undertaken, conscious that this modelling approach does not produce the fidelity and precision of other modelling methods, such as CFD modelling. However, it has been argued that the precision of the model is only as valuable as the quality of its inputs [19] (i.e. a 'consistent crudeness'), and thus that zone modelling provides a reasonable fidelity in the context of both the experimental data and the design information which is commonly available to fire engineers. The adoption of zone modelling also provides greater flexibility for fire engineers by not restricting the consideration of the electronic nozzle system exclusively to high-fidelity, complex modelling tools.

Further work will be needed to assess the introduction of water droplets in the modelling domain and how these may interact with the fire, impact the HRR, etc., since this will be an important consideration for fire engineers. However, this is beyond the scope of this paper and is part of planned future research.

3.2. Modelling tool

The modelling has been undertaken using B-RISK [5] version 2020.03. Incorporated into B-RISK is an underlying zone model used to calculate fire dynamics, smoke dispersion and temperature throughout
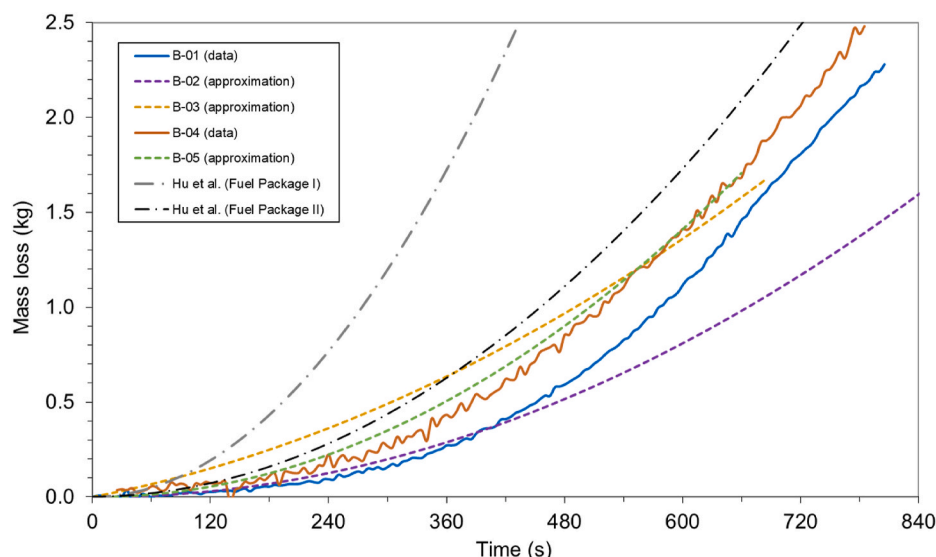

Fig. 8. Crib mass loss data used for the simulations.

enclosures, with each enclosure divided into two (upper and lower) gas layers. The fundamental equations are implemented as a system of differential equations which are solved to give outputs such as layer height, visibility and layer temperature. B-RISK includes well-validated sub-models for estimating the time of sprinkler activation, including the NIST/JET ceiling jet model [20].

B-RISK has been supported by multiple benchmarking studies which have focussed on sprinkler activation times in fire-affected enclosures. Wade et al. [21] and Hopkin and Spearpoint [22] have demonstrated that B-RISK provides a reasonable estimation of sprinkler activation times. Hopkin and Spearpoint [6] also adopted the tool in the consideration of concealed sprinkler head activation in a BS 9252:2011 [11] standard thermal response room test.

3.3. Representing the fuel package

For Series A, the HRR has adopted the lower bound of the range specified by Hostikka et al. [15]. This has been used as initial investigations found that it provides closest agreement between the temperatures observed in the tests and those estimated in the simulations (not presented herein for brevity). A value for the effective heat of combustion for foam slabs has also been adopted from Hostikka et al. [15], with a soot yield and a radiative fraction for polyurethane foam [23]. The burner area represented the combined area of the wood crib and two foam slabs of the fuel package (Section 2.1.2), while the elevation aligns with the midpoint of the foam slabs and the top of the wood crib.

In the Series B, the HRR has been estimated as a function of the mass loss rate measured from the load cell and assumed properties for the effective heat of combustion. The results for this are presented later in Section 4.2. It was not possible to identify when the PMMA ignited nor its proportional contribution to the fire at any given instant. The heat of combustion for Fuel Package I aligns with properties for Scots Pine [24]. For Fuel Package II, an assumed mass-weighted value of 18 200 kJ/kg has been adopted, assuming the heat of combustion of PMMA to be 26 200 kJ/kg [25]. The wood and PMMA properties used in this study were both selected from a previous B-RISK simulation study [26]. The burner area and elevation representing the size and location of the crib, a soot yield of 0.015 kg/kg for wood, a soot yield of 0.022 kg/kg for PMMA and a radiant fraction of 0.30 were applied to the Series B simulations. The mass-weighted soot yield for Fuel Package B is 0.0154 kg/kg.

Table 1 presents the fire parameters adopted for the modelling of the different experimental series and fuel packages.

3.4. Representing the suppression systems

To estimate the activation time of sprinkler heads, B-RISK applies the differential equation of Heskestad and Bill [27], which considers the interaction of the ceiling jet with the heat-responsive element. In estimating the activation time, empirical parameters are specified for the

Table 1
Fire properties adopted to represent the different fuel packages.

Parameter	Series A	Series B	
		Fuel Package I	Fuel Package II
HRR [kW]/Mass loss [kg]	Refer to Fig. 4	Refer to Fig. 8	Refer to Fig. 8
Burner area [m × m]	1.075 × 1.075	0.305 × 0.305	0.305 × 0.305
Burner elevation from floor level [m]	0.4	0.1	0.1
Soot yield [kg/kg]	0.227	0.0150	0.0154
Effective heat of combustion [kJ/kg]	22 700	17 750 [24]	18 200
Radiative fraction [−]	0.46	0.30	0.30

sprinkler heads, namely the response time index (RTI) and conductivity factor (C factor). The RTI represents the thermal time constant for the heat-responsive element in relation to velocity and convective heat transfer, while the C factor characterises the heat loss to the sprinkler housing due to conduction [6]. B-RISK has different means of estimating the ceiling jet parameters, i.e. velocity and gas temperature. Previous studies determined that this NIST/JET model [20] provides a closer estimation of sprinkler activation times compared to experimental data than Alpert's correlation [21,22], and therefore the NIST/JET model has been adopted in this paper.

Given the complexities associated with representing the electronic nozzle system in a simple zone model, an approach has been taken whereby it is assumed the system operates in a similar fashion to a sprinkler system. 'Effective' values have then been determined for the response time index (RTI) and conductivity factor (C factor) by a calibration exercise. The purpose of this calibration is to provide reasonable agreement to the experimental data. The calibrated parameters are presented in Table 2.

The Series B experiments include concealed residential sprinkler heads as well as the watermist automatic nozzles. Hopkin and Spearpoint [6] identified the relationship between RTI and C factor necessary to pass the BS EN 12259-14 [28] thermal response room test used for concealed heads, ultimately recommending an RTI of 290 $m^{1/2}s^{1/2}$ and a C factor of 0.5 $m^{1/2}s^{-1/2}$. In order to simulate the activation of the concealed heads, these values have been applied.

In each instance, the radial distance has been approximated as the distance from the centreline of the fire to the detection element (i.e., the nozzle or sprinkler head). A ceiling offset of 20 mm has been adopted throughout for a typical glass bulb [23], noting that this is not representative of the actual configuration. Finally, it has been assumed that the 'effective' rated temperature of the electronic nozzle system corresponds to the rated temperature of 68 °C for the concealed sprinkler head. This 'effective' temperature could have been varied along with the RTI and C factor, but this would have added more complexity to the analysis without providing any tangible benefits.

3.5. Room ventilation

The Series A experiments incorporate various natural openings as well as the inclusion of a mechanical fan in some instances. Each arrangement incorporates two full height (2.5 m) openings (Fig. 2). For these openings, a coefficient of discharge of 1.0 has been applied in the modelling, assuming no aerodynamic losses through the opening. This value is recommended in the B-RISK user guide [5] when the top of the opening is flush with the ceiling.

For the arrangements incorporating a fan, BS 8458 specifies a ventilation test be undertaken, where it is stated that at least one test should be repeated with the ambient air achieving a minimum velocity of 1 m/s. This velocity is measured inside the room at a location positioned 1 m above floor level and at a horizontal distance of 1 m from the fan. The fan itself is 500 mm in diameter and mounted with its horizontal central axis located 1 m above and parallel to the floor. For the purposes of this assessment, it is assumed that the fan achieves a volumetric supply flow rate of 0.2 m^3/s, based on a velocity at the fan of 1 m/s and a fan area of 0.2 m^2 (for a circular fan area with a diameter of 500

Table 2
'Effective' sprinkler head properties used to represent different activation elements.

Parameter	Electronic nozzle	Concealed sprinkler
Ceiling offset [mm]	20	
Ambient temperature [°C]	20	
Rated temperature [°C]	68	
RTI [$m^{1/2}s^{1/2}$]	20	290
C factor [$m^{1/2}s^{1/2}$]	0.25	0.5

mm).

From a series of sensitivity analyses undertaken for Exp. A-08, the mechanical ventilation is shown to have a negligible impact on the observed simulation outputs. This is due to how B-RISK captures fan interaction with the smoke layer and the height that the fan sits relative to the smoke layer (i.e., the fan is positioned below the observed upper smoke layer). This interaction, and its simplified representation in B-RISK, will likely warrant further investigation in future but is beyond the scope of this paper.

3.6. Surface properties

Table 3 provides a summary of the surface properties adopted for the modelling of the geometry. The gypsum plasterboard surfaces are based on properties defined by Hopkin et al. [29] and slabs have been simulated with concrete properties estimated from BS EN 1992-1-2:2004 [30]. The same surface properties have been adopted for the modelling of both experimental series.

4. Experimental results

4.1. Series A

A summary of the Series A results is given in Table 4, noting that one of the BS 8458 Annex C acceptance criteria is that the temperature 75 mm below the underside of the ceiling must not exceed 320 °C. From the experimental results it can be observed that the system demonstrates a relatively quick activation time, ranging from 52 s up to 84 s (01:24).

4.2. Series B

Fig. 8 shows the mass of the crib obtained from the experiments. In three of the experiments the load cell exhibited extensive signal noise, therefore the mass is shown as a best-fit approximation rather than the raw data. To illustrate the relative magnitude of the crib fires, using the previously selected values for the heat of combustion and the measured mass loss rates gives HRR values of between around 50 kW and 85 kW after 600 s compared to 1055 kW from the standardised Slow growth alpha t-squared fire [31].

Hietaniemi et al. [32] report the HRR from four refrigerator-freezer fire experiments in which the appliances were ignited by a 1 kW propane gas burner placed in the centre of the compressor motor space. In the case of the two free-standing appliances the HRR reached around 100 kW and 700 kW after 600 s. In the two experiments in which the appliance was housed within a melamine-faced particleboard cupboard the measured HRRs at 600 s were around 80 kW and 250 kW. Therefore, the cribs used in this work appear to correspond to a representative lower bound HRR.

Fig. 8 also shows the expected mass loss of the two crib designs using the method given by Hu et al. [33]. The method has been modified here as Hu et al.'s approach assumes the crib is ignited at the centre of the crib base whereas in these experiments the crib was simultaneously ignited at two neighbouring corners. In the case of a crib ignited in one corner it would appear reasonable to reduce the calculated mass loss using Hu

et al. by one quarter, and thus in the case of two corners to reduce the mass loss by a half. As expected, the method of Hu et al. predicts that the crib with the additional stick per layer (i.e. Fuel Package II) will burn more slowly. Mass loss results from Fuel Package II correspond to the prediction, however results from the single experiment that used Fuel Package I (B-01) shows a similar mass loss to the remaining experiments and therefore does not follow the predicted curve.

The measured activation times from the experiments are reported in Table 5. Experiment B-04 obtained the quickest measured activation time as might have been expected given the crib in this case was not concealed. When comparing the experimental results for the nozzles to the concealed sprinkler heads, in all instances the nozzles are shown to activate more quickly than the concealed heads. The activation times of the concealed head is shown to be between 2.0 and 13.7 times greater than those observed for the activation of the first nozzle.

5. Simulation results

Fig. 9 shows the comparison between the measured and simulated activation of the concealed residential sprinklers. The results suggest that the parameters previously proposed by Hopkin and Spearpoint [6] are sufficient to represent the activation time of the sprinklers. Fig. 9 also shows the simulated activation time of the electronically controlled nozzles for Series A and Series B. Given the faster activation times obtained in Series A, the results are replicated in an expanded region.

Five of the Series A experiments result in comparable match between the measured and simulated electronically controlled nozzle activation times. However, in three cases the calculated activation time is noticeably earlier than measured in the experiment (A-01, A-05 and A-08). These three experiments are where the fire was located in the corner of the enclosure. A potential reason why the simulation under-predicts the activation time is because the distance from the fire to the sensor is relatively short, but this does not address the geometrical arrangement where the fire and sensor are adjacent to the wall. To get a closer match between the measured and simulated activation times the results suggest that one solution would be to determine alternative 'equivalent' values for the RTI and/or C factor for this scenario. However, having different activation characteristics that depend on the fire location it not generally a practical approach to address this limitation. Another possible solution would be to increase the radial distance to some 'equivalent' length, although this approach has not been pursued for this paper.

When comparing the measured and calculated activation times of the electronically controlled nozzles in Series B the results show that the calculated times are all in excess of the measured times. On average the prediction is 1.8 times the measured value, and in the case of Experiment B-04 the difference is a large as a factor of 2.4 times.

In selecting the activation characteristics for the electronically controlled nozzles a balance has been struck between obtaining reasonable calculated times in the two series. In order to improve the match in Series A would then mean impractically long activation times would be determined for Series B. On the other hand, bringing the calculated times closer to the Series B experiments would mean the Series A calculated activation times would be likely deemed to be too optimistic. Given the objective of this work to assess scenarios that involve slower growing, shielded fires it is considered more critical to focus on the Series B experiments where the predictions exceed the measured values rather than the Series A experiments. It is also important to note that the Series A experiments represent 'Ultra-fast' growing fires, which may not typically be expected in a residential situation.

6. Discussion and conclusions

The fire source used in the BS 8458 test gives a more rapid fire development than the crib used in the Series B described in this paper. The intent in Series B was to simulate a refrigerator which burns significantly slower and with more smoke output than the fire source

Table 3
Geometry surface properties.

Parameter	Materials	
	Concrete	Gypsum plasterboard
Surface	Slab	Walls and ceilings
Thickness	100 mm	12.5 mm
Density	2300 kg/m^3	780 kg/m^3
Specific heat	0.9 kJ/kg/K	0.95 kJ/kg/K
Thermal conductivity	1.4 W/m/K	0.25 W/m/K
Emissivity	0.7	0.7

Table 4
Experimental results for Series A.

Exp.	Fire location[a]	Nozzle arrangement[b]	Fan ventilated[c]	Nozzle activation time [mm:ss]	First nozzle to activate[d]	Temperature 75 mm below ceiling [°C]
A-01	Corner	Arrangement 1	No	01:24	2	109
A-02	Centre 1	Arrangement 1	No	01:08	1	270
A-03	Centre 2	Arrangement 1	No	00:54	1	139
A-04	Centre 1	Arrangement 1	Yes	01:06	1	219
A-05	Corner	Arrangement 2	No	01:14	1	100
A-06	Centre 1	Arrangement 2	No	00:58	2	92
A-07	Centre 2	Arrangement 2	No	00:52	2	104
A-08	Corner	Arrangement 2	Yes	01:06	1	90

[a] Procedure considered three different fire locations, two located centrally and one in the corner.
[b] Procedure considered two different nozzle arrangements within the enclosure.
[c] Procedure considered the impact of variation in ambient air velocity conditions by incorporating a mechanical fan in certain arrangements.
[d] Each experiment incorporated two nozzles.

Table 5
Experimental results for Series B.

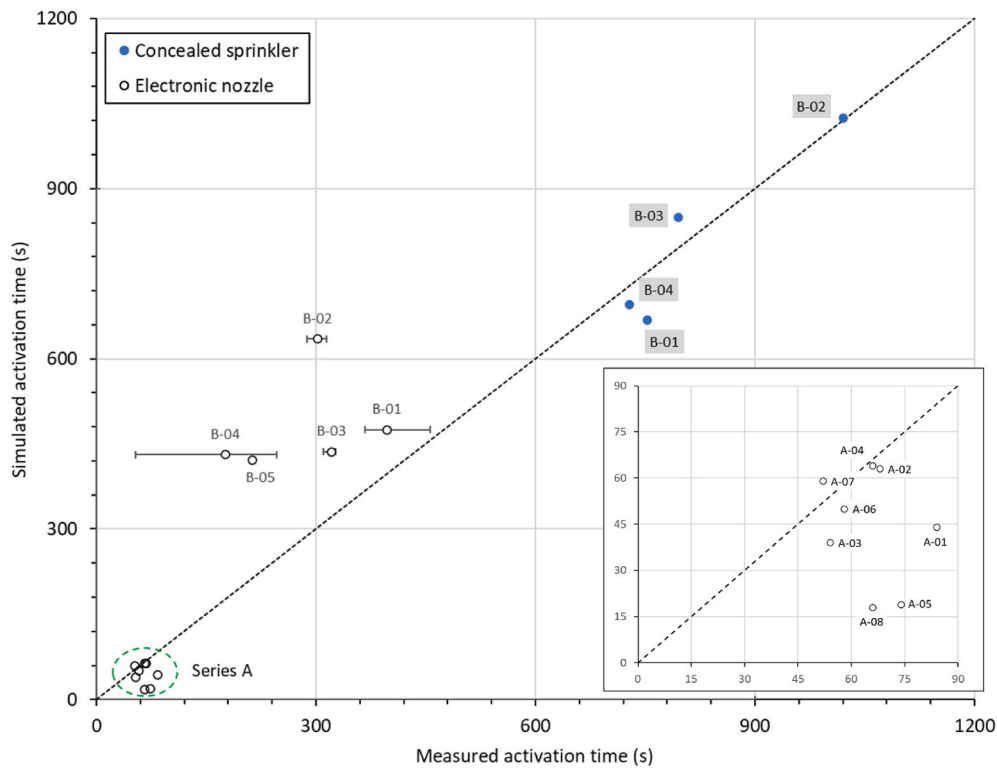| Exp.	Fuel Package	Fridge	Suppression	Sprinkler [mm:ss]	Nozzle 1 [mm:ss]	Nozzle 2 [mm:ss]	Nozzle 3 [mm:ss]
B-01	I	Yes	n/a	12:30	07:36	06:09	06:07
B-02	II	Yes	n/a	17:00	05:04	05:14	04:48
B-03	II	Yes	Sprinkler	13:15	05:27	05:27	05:10
B-04	II	No	Sprinkler	12:08	04:06	03:50	00:53
B-05	II	Yes	Electronic nozzle	–	–	03:33	–

Fig. 9. Comparison between measured and simulated activation times. Measured times are shown as a range where multiple results are available, inset expands Series A region.

used to assess suppression systems within standards. Although the objective was met, further development is required to assess the correspondence of the fire source with white goods-based fire scenarios.

The electronic nozzle system exhibited much more rapid activation times in the Series A experiments as a result of the more severe fire growth when compared to Series B. In Series A the corner fire location illustrated how this is a more challenging activation configuration and further development is being considered on how to improve its

performance. Furthermore, for the specific experiments presented in this paper the measured activation times of a concealed sprinkler head are 2.0–13.7 times greater than those using an electronic nozzle system.

Simulated activation times of concealed sprinklers using the recommendations of Hopkin and Spearpoint [6] show a good match with the measured times. The correspondence is similar whether the fire was concealed or not.

A combination of an effective RTI of 20 $m^{1/2}s^{1/2}$ and an effective C

factor of 0.25 m$^{\frac{1}{2}}$s$^{-\frac{1}{2}}$ has been shown to reasonably predict activation times for an electronic nozzle system when simulated in the B-RISK zone model. Using these characteristics found that the simulated activation times of the Series B enclosure fires were on average twice as slow as the measured activation times. This may partly have been because of the concealed nature of the fire although this finding is also the case even where the fire was not concealed. For the BS 8458 test arrangement the B-RISK predictions were on average 1.4 times quicker than the measured times. When the fire was in its corner location the simulated activation of the electronic nozzle system exhibited noticeably earlier times (around 2.5 times sooner) than measured in the experiment. Investigating whether an adjusted 'effective' radial distance would be a viable approach to increase the predicted activation times may be appropriate. Where the fires were away from the corner of the enclosure the B-RISK predictions were on average 11% quicker than the measured times. Combining all of the results from the two experimental series gives an overall average difference of 14% slower activation time predictions from B-RISK.

Further work is ongoing to determine the hazard presented by the Series B fires and to compare how that hazard is altered by the use of a concealed sprinkler and the electronic nozzle system. The intent is to also undertake a comparison between the hazard developed in the experiments with B-RISK zone model predictions.

Author statement

Michael Spearpoint: Conceptualisation, Writing - Original Draft, Formal analysis, Visualisation.

Charlie Hopkin: Conceptualisation, Writing - Original Draft, Formal analysis, Visualisation.

Yusuf Muhammad: Conceptualisation, Writing - Review & Editing, Investigation, Resources, Funding acquisition.

William Makant: Conceptualisation, Writing - Review & Editing, Investigation, Resources, Funding acquisition.

Funding

Declaration of competing interest

Authors of this work include individuals who are involved in the product development and sale of watermist systems with electronically controlled nozzles.

References

[1] R. Chagger, 'The Causes of Fire Fatalities and Serious Fire Injuries in Scotland and Potential Solutions to Reduce Them - Phase 1: IRS Review', BRE Trust, Briefing Paper, Watford, UK, 2019.

[2] Effectiveness of Sprinklers in Residential Premises, Executive Summary, Building Research Establishment, Garston, UK, 2005. , BRE report number 204505.

[3] W.L. Grosshandler, D. Lowe, K. Notarianni, W. Rinkinen, Protection of Data Processing Equipment with Fine Water Sprays, National Institute of Standards and Technology, Gaithersburg, MD, 1994. , NISTIR 5514.

[4] BSI, BS 8458:2015 Fixed Fire Protection Systems. Residential and Domestic Watermist Systems. Code of Practice for Design and Installation, BSI, London, 2015.

[5] C. Wade, G. Baker, K. Frank, R. Harrison, M. Spearpoint, B-RISK 2016 User Guide and Technical Manual, SR364, Building Research Association of New Zealand, 2016.

[6] C. Hopkin, M. Spearpoint, Numerical simulations of concealed residential sprinkler head activation time in a standard thermal response room test, Building Services Engineering Research and Technology, 2020, https://doi.org/10.1177/0143624420953302.

[7] Z.L. Magnone, J. Crocker, P. Peña, 'Warehouse Protection of Exposed Expanded Group-A Plastics with Electronic Sprinkler Technology', Presented at the 16th International Conference on Automatic Fire Detection, AUBE'17, Hyattsville, MD, USA, 2017. Sep.

[8] S. Kopylov, L. Tanklevskiy, M. Vasilev, V. Zima, A. Snegirev, Advantages of electronically controlled sprinklers (ECS) for fire protection of tunnels, in: Proceedings from the Fifth International Symposium on Tunnel Safety and Security, Mar., New York, USA, 2012, pp. 87–92.

[9] Plumis fire suppression'. https://plumis.co.uk/.

[10] BSI, BS EN 520:2004+A1:2009 Gypsum Plasterboards. Definitions, Requirements and Test Methods, British Standards Institution, London, 2004.

[11] BSI, BS 9252. Components for Residential Sprinkler Systems. Specification and Test Methods for Residential Sprinklers, BSI, London, 2011.

[12] BSI, BS EN 12259-14. Fixed Firefighting Systems. Components for Sprinkler and Water Spray Systems, Sprinklers for residential applications, London, 2020. BSI

[13] UL, UL 1626. Standard for Safety for Residential Sprinklers for Fire-Protection Service, Fourth Edition, Underwriters Laboratories Inc., 2008.

[14] R.G. Bill, H.-C. Kung, S.K. Anderson, R. Ferron, A new test to evaluate the fire performance of residential sprinklers, Fire Technol. 38 (2) (2002) 101–124, https://doi.org/10.1023/A:1014407200101.

[15] S. Hostikka, E. Veikkanen, T. Hakkarainen, T. Kajolinna, Experimental investigation of human tenability and sprinkler protection in hospital room fires, Fire Mater. 45 (6) (2021) 823–832, https://doi.org/10.1002/fam.2893.

[16] N. Elsagan, Y. Ko, A Parametric Study of Numerical Modelling of Water Mist Systems in Protection of Wood Frame Buildings, Wood & Fire Safety, Cham, 2020, pp. 166–172, https://doi.org/10.1007/978-3-030-41235-7_25.

[17] K. McGrattan, S. Hostikka, R. McDermott, J. Floyd, M. Vanella, Fire Dynamics Simulator User's Guide, National Institute of Standards and Technology, Gaithersburg, MD, 2019, https://doi.org/10.6028/NIST.SP.1019. ,NIST SP 1019,.

[18] T. Rappsilber, S. Krüger, Design fires with mixed-material burning cribs to determine the extinguishing effects of compressed air foams, Fire Saf. J. 98 (2018) 3–14, https://doi.org/10.1016/j.firesaf.2018.03.004.

[19] D.G. Elms, Consistent crudeness in system construction, in: B.H.V. Topping (Ed.), Optimization and Artificial Intelligence in Civil and Structural Engineering: Volume I: Optimization in Civil and Structural Engineering, Springer Netherlands, Dordrecht, 1992, pp. 71–85, https://doi.org/10.1007/978-94-017-2490-6_6.

[20] W. Davis, The Zone Fire Model Jet: a Model for the Prediction of Detector Activation and Gas Temperature in the Presence of a Smoke Layer, National Institute of Standards and Technology, Gaithersburg, MD, 1999. NISTIR 6324.

[21] C. Wade, M. Spearpoint, A. Bittern, K. Tsai, Assessing the sprinkler activation predictive capability of the BRANZFIRE fire model, Fire Technol. 43 (3) (2007) 175–193, https://doi.org/10.1007/s10694-007-0009-5.

[22] C. Hopkin, M. Spearpoint, Evaluation of sprinkler actuation times in FDS and B-RISK, Int. Fire Prof. J. 28 (2019) 22–27.

[23] C. Hopkin, M. Spearpoint, A. Bittern, Using experimental sprinkler actuation times to assess the performance of Fire Dynamics Simulator, J. Fire Sci. 36 (4) (2018) 342–361, https://doi.org/10.1177/0734904118772306.

[24] M. Aniszewska, A. Gendek, W. Zychowicz, Analysis of selected physical properties of conifer cones with relevance to energy production efficiency, Forests 9 (7) (2018), https://doi.org/10.3390/f9070405.

[25] D. Drysdale, An Introduction to Fire Dynamics, third ed., John Wiley & Sons, Ltd, 2011 https://doi.org/10.1002/9781119975465.ch1.

[26] S. Sazegara, M. Spearpoint, G. Baker, Benchmarking the single item ignition prediction capability of B-RISK using furniture calorimeter and room-size experiments, Fire Technol. 53 (4) (2017) 1485–1508, https://doi.org/10.1007/s10694-016-0642-y.

[27] G. Heskestad, R.G. Bill, Quantification of thermal responsiveness of automatic sprinklers including conduction effects, Fire Saf. J. 14 (1) (1988) 113–125, https://doi.org/10.1016/0379-7112(88)90049-5.

[28] BSI, BS EN 12259-14. Fixed Firefighting Systems. Components for Sprinkler and Water Spray Systems. Sprinklers for Residential Applications, BSI, London, 2020.

[29] D. Hopkin, T. Lennon, J. El-Rimawi, V. Silberschmidt, A numerical study of gypsum plasterboard behaviour under standard and natural fire conditions, Fire Mater. 36 (2) (2012) 107–126, https://doi.org/10.1002/fam.1092.

[30] BSI, EN 1992-1-2:2004+A1:2019 Eurocode 2. Design of Concrete Structures, General rules. Structural fire design', London, 2005. BSI.

[31] BSI, PD 7974-1. Application of Fire Safety Engineering Principles to the Design of Buildings. Initiation and development of fire within the enclosure of origin (Sub-system 1), BSI, London, 2019.

[32] J. Hietaniemi, J. Mangs, T. Hakkarainen, Burning of Electrical Household Appliances : an Experimental Study, VTT Research, Espoo, Finland, 2001. Note 2084.

[33] L.H. Hu, Y.Z. Li, H.B. Wang, R. Huo, An empirical equation to predict the growth coefficient of burning rate of wood cribs in a linear growth model, J. Fire Sci. 24 (2) (2006) 153–170, https://doi.org/10.1177/0734904106056600.